Author Manuscript

Author Manuscript

Author Manuscript

Author Manuscript

HHS Public Access

Author manuscript

Nature. Author manuscript; available in PMC 2015 November 28.

Published in final edited form as:

Nature. 2015 May 28; 521(7553): 520–524. doi:10.1038/nature14269.

Global genetic analysis in mice unveils central role for cilia in congenital heart disease

You Li[1,8], **Nikolai T. Klena**[1,8], **George C Gabriel**[1,8], **Xiaoqin Liu**[1,7], **Andrew J. Kim**[1], **Kristi Lemke**[1], **Yu Chen**[1], **Bishwanath Chatterjee**[1], **William Devine**[2], **Rama Rao Damerla**[1], **Chien-fu Chang**[1], **Hisato Yagi**[1], **Jovenal T. San Agustin**[5], **Mohamed Thahir**[3,4], **Shane Anderton**[1], **Caroline Lawhead**[1], **Anita Vescovi**[1], **Herbert Pratt**[5], **Judy Morgan**[6], **Leslie Haynes**[6], **Cynthia L. Smith**[6], **Janan T. Eppig**[6], **Laura Reinholdt**[6], **Richard Francis**[1], **Linda Leatherbury**[7], **Madhavi K. Ganapathiraju**[3,4], **Kimimasa Tobita**[1], **Gregory J. Pazour**[5], and **Cecilia W. Lo**[1,9]

[1]Department of Developmental Biology, University of Pittsburgh School of Medicine, Pittsburgh, PA

[2]Department of Pathology, University of Pittsburgh School of Medicine, Pittsburgh, PA

[3]Department of Biomedical Informatics, University of Pittsburgh School of Medicine, Pittsburgh, PA

[4]Intelligent Systems Program, School of Arts and Sciences, University of Pittsburgh, Pittsburgh, PA

[9]Corresponding author. cel36@pitt.edu Phone: 412-692-9901, Mailing address: Dept of Developmental Biology, Rangos Research Center, 530 45th St, Pittsburgh, PA, 15201.

[8]Co-first authors

Author Contributions: Study design: CWL
ENU mutagenesis, line cryopreservation, JAX strain datasheet construction: HP, LR, JM, LH
Mouse breeding, sample collection, sample tracking: SA, CL, KL, GCG, AV, CWL
Electronic database construction and maintenance: CC
MGI curation: KT, GCG, LL, CWL, CLS, JTE,
CHD phenotyping: XL, KL, YC, GCG, AJK, SA, WD, CWL, LL, KT, RF
Cilia immunostain and histology: JTS, GJP, RF
Analysis of airway and node cilia motility: RF, KL, GCG, AJK
Exome sequencing analysis: YL
Mutation validation: NTK, BC, RD, HY, YL
Mutation mapping: RD, NTK, BC, YL
Interactome analysis: MKG, MT
Ciliome and pathway annotation: CWL, GJP, GCG, NTK, YL
Manuscript preparation: CWL, YL, NTK, GCG

[1]**Author Information**: All mutant mouse lines recovered in this mouse mutagenesis screen and theirphenotype description and causative mutations are curated in the Mouse GenomeInformatics (MGI) database (www.informatix.jax.org) and can be retrieved from MGI byentering "b2b" in the search box.

[2]All mutant mouse lines curated in MGI can be reanimated from sperm cryopreserved in the Jackson Laboratory (JAX®Mice) Repository.

[3]All mutations recovered by mouse exome sequencing analysis are searchable together with phenotype information via the public Bench to Bassinet Congenital Heart Disease Mouse Mutation Database (http://benchtobassinet.com/ForResearchers/BasicScienceDataResourceSharing/GeneDiscoveryinMouseModels.aspx)

[4]The mouse exome datasets are available from the GNomEx CardiovascularDevelopment Consortium (CvDC) Datahub (https://b2b.hci.utah.edu/gnomex/gnomexGuestFlex.jsp?topicNumber=67)

Supplemental Information: A. Extended data figure legends
B. Supplemental spreadsheets
C. Supplemental movie legends.

Author Manuscript Author Manuscript Author Manuscript Author Manuscript

[5]Program in Molecular Medicine, University of Massachusetts Medical School, Worcester, MA

[6]The Jackson Laboratory, Bar Harbor, ME

[7]The Heart Center, Children's National Medical Center, Washington, D.C

Abstract

Congenital heart disease (CHD) is the most prevalent birth defect, affecting nearly 1% of live births[1], but the incidence of CHD is up to ten fold higher in human fetuses[2,3]. A genetic contribution is strongly suggested by the association of CHD with chromosome abnormalities and high recurrence risk[4]. Here we report findings from a recessive forward genetic screen in fetal mice, showing the cilium and cilia transduced cell signaling play important roles in the pathogenesis of CHD. The cilium is an evolutionarily conserved organelle projecting from the cell surface with essential roles in diverse cellular processes. Using echocardiography, we ultrasound scanned 87,355 chemically mutagenized C57BL/6J fetal mice and recovered 218 CHD mouse models. Whole exome sequencing identified 91 recessive CHD mutations in 61 genes. This included 34 cilia-related genes, 16 genes involved in cilia transduced cell signaling, and 10 genes regulating vesicular trafficking, a pathway important for ciliogenesis and cell signaling. Surprisingly, many CHD genes encoded interacting proteins, suggesting an interactome protein network may provide a larger genomic context for CHD pathogenesis. These findings provide novel insights into the potential Mendelian genetic contribution to CHD in the fetal population, a segment of the human population not well studied. We note pathways identified show overlap with CHD candidate genes recovered in CHD patients[5], suggesting they may have relevance to the more complex genetics of CHD overall. These CHD mouse models and >8,000 incidental mutations are sperm archived, creating a rich public resource for human disease modeling.

Inbred C57BL/6J mice mutagenized with ethylnitrosourea (ENU) were bred to recover recessive coding mutations (Extended Data Fig. 1). Phenotyping was conducted using noninvasive fetal echocardiography, an ultrasound imaging modality also employed clinically for CHD diagnosis. This unbiased study design allows detection of even those CHD mutants inviable to term[6], a segment of CHD cases that would be largely clinically inaccessible for genetic analysis. Using combination of color flow, 2D, spectral Doppler and M-mode imaging, a wide spectrum of CHD phenotypes were recovered, including cardiac looping defects, OFT malalignment/septation defects, ventricular/atrioventricular septal defects, and various right/left heart obstructive lesions[6] (Figure 1; Supplemental Movies S1-S3). The CHD diagnoses were confirmed with microCT/microMRI, necropsy, and histopathology (Extended Data Fig. 1). Heritability was ascertained with recovery of two or more G3 fetuses with the same CHD phenotype (n=4.6±2.6). Ultrasound scanning of 87,355 G3 fetuses from 2,651 mutant lines (defined by the G1 sire) recovered 218 CHD mutant lines. These were curated in the Mouse Genome Informatics Database (http://www.informatics.jax.org/searchtool/Search.do?query=b2b&submit=Quick%0D%0ASearch), with G1 sperm cryopreserved in the Jackson Laboratory (JAX®Mice).

Many mutant lines (30%) exhibited complex CHD associated with heterotaxy, the randomization of left-right patterning. These heterotaxy mutants often died prenatally. We note clinical studies show 16% of human fetuses with complex CHD have heterotaxy[7], and

Author Manuscript Author Manuscript Author Manuscript Author Manuscript

these also exhibit high prenatal/intrauterine death (30-60%)[8,9]. Also commonly observed in mutant lines with or without laterality defects are double outlet right ventricle (DORV) and atrioventricular septal defects (AVSD), phenotypes that usually resulted in prenatal lethality. We note DORV and AVSD are also observed with high prevalence in aborted/stillborn human fetuses[3]. Most heterotaxy mutant lines exhibited three distinct visceral organ situs phenotypes: normal situs solitus, mirror symmetric situs inversus, or randomization with heterotaxy, with complex CHD observed only with heterotaxy (Extended Data Fig. 2). These three phenotypes are found in patients and mice with mutations causing primary ciliary dyskinesia (PCD)[10,11], a sinopulmonary disease arising from immotile/dyskinetic respiratory cilia. This reflects the common requirement for motile cilia in airway clearance and left-right patterning[11,12]. Hence, we conducted videomicroscopy of the tracheal epithelia to assess cilia motility as a proxy for the node.

Mutation recovery was conducted with whole exome sequencing analysis of a single mutant from each of 113 mutant lines. Cumulatively this yielded 7,996 coding mutations in 4,809 genes (Extended Data Fig. 3a). Genotyping analysis identified the pathogenic mutation as one consistently homozygous across all G3 mutants bearing the same phenotype. In mutant lines with multiple homozygous mutations on the same chromosome linked to the CHD phenotype, the pathogenic mutation was identified with segregation analysis of additional mutants, and/or based on phenotype comparison to existing knockout/mutant alleles. For five lines (b2b002/b2b012/b2b284/b2b1519/b2b1146), the mutation was confirmed with mapping analyses[13].

In this manner, 91 pathogenic mutations were recovered in 61 genes (Supplemental Spreadsheet 1). The distribution of missense/splicing/nonsense mutations were similar to other ENU mutagenesis studies[14] (Extended Data Fig. 3a). All mutations except one were in highly conserved amino acids (Supplemental Spreadsheet 2). Five of the 19 splicing mutations are >2-bases from the canonical splice donor-acceptor sites, the farthest being 10 bases apart (*Dnah5*$^{c.13329\text{-}10T>A}$;b2b1537; validated by cDNA sequencing, Extended Data Fig. 4). Multiple alleles were recovered in 15 genes (Extended Data Table 1). Of 61 CHD genes recovered, 27 were not previously annotated to cause CHD (Extended Data Fig. 3b), either because no mutant/knockout mice were available, or the CHD phenotype was not investigated (Supplemental Spreadsheet 1). In some instances, the existing mutants died early, precluding CHD analysis, such as the *Smarca4* knockout mouse with peri-implantation lethality[15]. A *Hectd1* mutant was previously described only with neural tube defects[16] versus our *Hectd1*^{b2b327} mutant shown to have aortic atresia (Figure 1c,d). The identical *Adamts6* mutation was found in 3 lines, shown to be a spontaneous mutation in the C57BL6/J support colony (Supplemental Spreadsheet 1).

Thirty-four of the 61 CHD genes are cilia-related (Figure 2), 23 in laterality mutant lines (Extended Data Table 2, Fig.3a,5). Twelve are required for motile cilia function, with 8 clinically known to cause PCD and 3 likely novel PCD genes *(Ccdc151,Daw,Pkd1l1)* (Extended Data Tables 2,3; Supplemental Spread Sheet 1). A mutation was recovered in *Foxj1*, a transcription factor known to regulate ciliogenesis. While *Foxj1* knockout mice have no cilia in the airway[17], our *Foxj1*^{b2b774} mutant harboring a missense mutation in the

Author Manuscript Author Manuscript Author Manuscript Author Manuscript

DNA binding domain has ciliated trachea with robust ciliary motion (Supplemental Movie S4), but with no nodal flow (Supplemental Movie S5).

Mutations in 22 ciliome genes affect primary cilia - 11 in laterality and 11 in nonlaterality mutant lines (Extended Data Table 2, Fig. 3a,5). Among nonlaterality mutants are *Cep110* - centrosome component, *Jbts17* - cilia transition zone protein, and four other genes (*Fuz,Myh10,Dctn5,Lrp2)* that also play important roles in vesicular/endocytic trafficking, a biological process essential for ciliogenesis[18,19] (Figure 2). Many genes affecting laterality are associated with non-PCD ciliopathies *(Anks6,Bicc1,Tbc1d32, Cep290,Dync2h1,Ift74,Ift140,Nek8,Pcsk5,Pskh1,Cc2d2a,Tmem67;* Extended Data Table 3)[20,21]. Analysis of *Cc2d2a* mutant embryo by confocal imaging showed shorter and fewer cilia throughout the embryo (Figure 1s-x). In *Cc2d2a* mutant embryo, while cilia were abundant in outflow cushions, they were absent in AV cushions (Figure 1p,r). Consistent with this, *Cc2d2a* mutant embryos die prenatally with AVSD (Figure 1l,n), but with normal semilunar valves (Figure 1m,n).

Of the 26 non-ciliome CHD genes, 15 are known to mediate cell signaling, including SHH (*Fuz,Kif7,Lrp2,Sufu,Tbc1d32*), WNT/planar cell polarity (*Ptk7,Prickle 1,Fuz*), TGF-p/BMP (*Cfc1,Ltbp1,Megf8, Pcsk5,Smad6,Tab1*), and calcium signaling (*Pkd1l1,Pkd1*) (Figure 2). Five of these were recovered in the laterality mutant lines (*Tbc1d32,Cfc1,Megf8,Pcsk5,Pkd1l1*). These pathways are all transduced or modulated by the cilium, and play significant roles in cardiovascular development and/or left-right patterning.

We also recovered 10 CHD genes mediating vesicular/endocytic trafficking, including four (*Lrp2,Myh10,Dctn5*m*Fuz*) that are ciliome related (Figure 2). The enrichment for endocytic genes may be mechanistically linked to cilia, as vesicular trafficking at the cilia base has important roles in both ciliogenesis and cilia transduced cell signaling[18,19,22]. These endocytic genes caused a similar spectrum of OF malalignment and septation defects (Extended Data Fig. 6). Only *Ap1b1*, an adaptin subunit mediating endocytic protein sorting in the Golgi was observed to cause laterality defects (b2b1660; Extended Data Fig. 2). While *Ap1b1* mutants showed normal airway and embryonic node cilia motility (Supplemental Movie S6,S7), *Ap1b1* mutant embryonic fibroblasts exhibited ciliogenesis defect (65% vs. 85% ciliation in *Ap1b1* mutant versus wildtype fibroblasts;$p=5.90\times10^{-6}$). *Ap2b1*, an adaptin protein complex 2 subunit homologous to *Ap1b1*, functions in clathrin mediated endocytosis. *Snx17*, known to regulate endocytic receptor recycling, has a mutation in the cargo binding FERM domain, region known to interact with the NPXY motif of endocytic protein LRP1, which was also recovered in our screen (Extended Data Fig.3b).

Other CHD genes recovered included a novel zinc finger protein *Zbtb14*, and two genes modulating chromatin, *Smarca4* and *Prdm1*. Also recovered were six extracellular matrix related genes (*Acan,Adamts6, Frem2,Lox,Mmp21,Ndst1*), one (*Lox*) identified as cilia-related, three novel genes (*Cml5,Gm572,Mmp21*) causing *CHD* with laterality defects, and two genes (*Acan, Pkd1*) causing biventricular hypertrophy without other structural heart defects.

Author Manuscript Author Manuscript Author Manuscript Author Manuscript

Many of the CHD genes encode proteins known to physically interact or are in the same multiprotein complexes. For example, ANKS6 can bind BICC1 and also NEK8, with NEK8/ANKS6 colocalizing in the cilia inversin compartment[24,25]. TMEM67, CEP290, JBTS17, and CC2D2A are colocalized in the NPHP1-4-8 multiprotein complex in the cilia transition zone[23]. *DNAH5, DNAH11, DNAI1* and *DAW1* are associated with the outer dynein arm complex of motile cilia, while IFT140 and IFT74 are intraflagellar transport protein components that together with DYNC2H1 mediate protein transport in the cilium (Figure 2)[18,20]. SNX17 can directly bind LRP1 to promote LRP1 cell surface recycling[26]. These findings prompted an examination of the 113 exomes for the prevalence of additional mutations in the 61 CHD genes. This showed 58 additional incidental mutations in 32 of the CHD genes, a significant enrichment compared to random simulations (P=0.00114;Online Methods), suggesting possible modifier effects.

To further assess for potential protein-protein interactions (PPI), we constructed an interactome of CHD genes using known PPIs in the public databases and our own computationally predicted PPIs (Online Methods). This yielded an interactome of 778 genes, 292 are predicted PPIs (Supplemental Spreadsheet 3;Figure 3a). The average shortest distance between CHD genes is 4.3±2.5 edges, whereas random genes of matched degree distribution had a larger distance of 5.7±4.4 edges (P=0.01). Statistical analysis of the interactome revealed significant Go Ontology term enrichment related to development, including heart development terms (Supplemental Spreadsheet 3;Figure 3b). Pathways identified included “clathrin-mediated endocytosis signaling”, “TGFβ signaling”, “BMP signaling” and “axon pathfinding” (Supplemental Spreadsheet 3). Several CHD genes recovered are known to regulate axon guidance and neurogenesis, including *Plxnd1*, *Robo1*, and *Cxcr4*, while *Pde2a* regulates synaptic plasticity and long term potentiation, and *Myh10* is required for synaptic membrane recycling (Extended Data Fig.7).

Overall, our study provides compelling evidence that the cilium plays a critical role in CHD pathogenesis. The observed enrichment for cilia and cilia-related genes emerged from a phenotype driven forward genetic screen agnostic to the specific genes that may be recovered. The finding of ciliome mutations in CHD mutant lines with and without laterality defects would suggest a broad role for cilia in CHD pathogenesis. While our study is focused on monogenic recessive coding mutations, we noted striking overlap of genes recovered in the mouse screen versus heterozygous de novo coding mutations in CHD candidate genes identified in CHD patients[5]. Of 28 CHD genes identified in the human study - 11 are cilia-related, 7 are in TGFb/SHH/WNT signaling, and 2 in vesicular/endocytic trafficking (Supplemental Spread Sheet 4). Heterozygous mutation in *PITX2*, a gene essential for left/right patterning[12], was recovered in a non-heterotaxy CHD patient, suggesting a broader role for left-right patterning in CHD pathogenesis. The human study identified an important role for genes regulating chromatin. Consistent with this, our screen recovered two mouse CHD genes modulating chromatin, *Smarca4* and *Prdm1*[5]. Hence, findings from our fetal mouse screen may provide insights not only on Mendelian recessive genetic contribution to CHD in the unborn, a segment of the CHD population not well studied, but these findings also may have relevance to the complex genetics of CHD overall. The CHD mouse models generated in this study are invaluable resources for interrogating

Author Manuscript Author Manuscript Author Manuscript Author Manuscript

CHD pathogenesis, with the cryopreserved mutant lines providing access to a large library of mutations, including null mutations for genes without KOMP alleles.

Online Methods

Congenital Heart Defect Phenotyping

C57BL/6J mice were chemically mutagenized using ethylnitrosourea and subject to a two generation backcross breeding scheme[27]. To identify CHD mutants, G3 fetuses were ultrasound scanned with a two-tier ultrasound phenotyping strategy using the Acuson Sequoia and Vevo2100 ultrasound systems as previously described[6]. The fetal ultrasound imaging was conducted at E13.5-15.5, after completion of major cardiovascular developmental processes, including outflow tract septation and ventricular chamber septation. All of the CHD diagnoses were confirmed or refined by additional analysis using micro-CT/micro-MRI analyses and 3D histopathology using episcopic confocal microscopy[6,28] (Extended Data Figure 1). The summative CHD diagnosis and phenotype description are curated in the public Mouse Genome Informatics (MGI) database (www.informatix.jax.org; enter search box “b2b” will pull up all the lines or type in specific line ID or MGI ID to go directly to a specific mutant line). Included in each mutant line MGI record are sample images and videos collected from various different imaging modalities, including ultrasound images and videos, necropsy images, microCT/microMRI scans, episcopic confocal microscopy image stacks and 3D reconstructions, histology, and high speed videos for analysis of tracheal airway cilia motility.

Cilia Videomicroscopy

Trachea of newborn mice were harvested and mounted as previously described. For nodal cilia imaging, the node-containing region of E7.5-E7.75 embryos (3-6 somite stages) was dissected and mounted on a glass coverslip[10]. Videomicroscopy was carried out using a Leica DMIRE2 inverted microscope at 37°C with a 100× oil objective, and DIC optics. To examine flow, 0.35 μm microspheres were added to the medium bathing the ciliated tissue samples ($\sim 1 \times 10^{11}$ particles/ml, Polysciences, Inc.). High-speed videos (200 fps) were collected using a Phantom v4.2 camera (Vision Research, NJ).

Mutation Recovery with Whole Exome Sequencing Analysis

Genomic DNA from CHD mutant mice were sequence captured using Agilent SureSelect Mouse All Exon kit V1, and sequenced using Illumina HiSeq 2000 with minimum average 50× target sequence coverage (BGI Americas). Sequence reads were aligned to C57BL/6J mouse reference genome (mm9) and analyzed using CLCBio Genomic Workbench and GATK software. To minimize false-negatives, variant calls were set at 5× minimum coverage and >20% alternate reads. Sequence variants were annotated with annovar (http://www.openbioinformatics.org/annovar/) and filtered against dbSNP128 and our in-house mouse exome databases with custom scripts. Intronic variants within 10bp from the splice junction were annotated as potential splicing mutation. All of the mutations recovered are searchable together with phenotype information via the public Bench to Bassinet Congenital Heart Disease Mouse Mutation Database (http://benchtobassinet.com/ForResearchers/BasicScienceDataResourceSharing/GeneDiscoveryinMouseModels.aspx). The exome

Author Manuscript Author Manuscript Author Manuscript Author Manuscript

datasets are available from the GNomEx CvDC Datahub (https://b2b.hci.utah.edu/gnomex/gnomexGuestFlex.jsp?topicNumber=67).

Ciliome Gene Annotation

Ciliome genes were derived from a compilation of multiple bioinformatics, genomic and proteomic studies in different species[29]. This included a bioinformatics study of X-box containing genes in *C. elegans* and several proteomic and comparative genomic studies comprising ciliated organisms in several species (*C. elegans*, *Drosophila*, *Human*, *Chlamydomonas*, *Plasmodium falciparum* and *Trypanosoma*). In addition, we also included genes recently identified in the cilia transition zone complex[23] and genes identified to cause Primary Ciliary Dyskinesia (http://ghr.nlm.nih.gov/condition/primary-ciliary-dyskinesia/show/Related+Gene(s)).

Analysis of Splicing Defect Mutations

For analysis of splicing defect mutations, RNA was isolated from skin, trachea, or heart tissue and reverse transcribed to generate cDNA using a High Capacity RNA-to-cDNA Kit (Life Technologies, Inc.). PCR amplification of the cDNA was carried out with primers spanning the affected splice junction using AmpliTaq Gold™ DNA polymerase system (Life Technologies) (95°C for 5 min, 40 cycles at 95°C for 30 s, 58°C for 30 s at 72°C for 1 min, 72°C for 5 min). The amplified products were separated on a 3% agarose gel and the bands were excised using the QIAquick Gel Extraction Kit (Qiagen) and analyzed by Sanger capillary sequencing.

Simulation-based Mutation Enrichment Analysis

A simulation approach was used to test whether mutations in the 61 CHD genes are enriched in the mouse exome datasets generated from the 113 CHD mutant mouse lines. From the 113 exomes, we recovered 149 mutations in the 61 CHD genes, 91 of which were identified as pathogenic, yielding an excess of 58 incidental mutations. For this simulation, all the genes from the mouse genome were grouped in bins of 500 genes based on coding DNA sequence (CDS) length. Then 61 genes with the same size distribution as the observed 61 CHD genes were randomly sampled. For each bin that contained k of our 61 CHD genes, we randomly sampled k genes, and counted the number of mutations in these genes in the 113 mouse exomes. Based on 50,000 sets of 61 randomly sampled genes, we calculated a p-value based on the count of random gene sets that harbored 149 or more mutations. To take potential gene coverage bias into account, we limited our random gene selection to genes with at least one coding mutation in our CHD exomes, which yielded p-value of 0.00114. When we choose random genes from all genes, including genes not found in our exome dataset, p-value is <0.00002.

Interactome Analysis

To construct the interactome, each of the mouse CHD genes was mapped to its human ortholog, and PPIs of these genes were extracted from HPRD (www.hprd.org) and BioGRID (thebiogrid.org). The interactome is augmented with PPIs discovered computationally using the recently developed HiPPIP model (unpublished results). Pathway and Gene Ontology

Author Manuscript Author Manuscript Author Manuscript Author Manuscript

term enrichment analysis of the interactome were carried out using Ingenuity Pathway Analysis suite and BiNGO[30] plugin of Cytoscape (http://www.cytoscape.org/). P-value for each pathway and GO term was calculated using Fisher's exact test with Benjamini-Hochberg correction (Supplementary Spread Sheet 3). Shortest paths were computed using Dijkstra's algorithm implemented in the networkx package of python. Average length of the shortest paths between pairs of CHD genes was compared to that of 61 random genes, where random genes were sampled to have similar degree distribution as the 61 CHD genes. For this, all human genes were categorized into 7 bins based on their degree in the interactome, (0, 1-5, 6-25, 26-50, 51-75, 75-100, >100). As many random genes were selected from any bin as the number of CHD genes in that bin. This process was repeated 1,500 times, and average length of the shortest paths is computed each time. P-value is computed empirically to determine statistical significance.

Extended Data

Extended Data Table 1
CHD Genes with Multiple Alleles

Gene Symbol (mouse)	Gene Symbol (human)	Mouse CDS (bp)	# Alleles Recovered
Daw1	***DAW1***	933	2
Dnai1	***DNAI1***	2,106	2
Drc1	***DRC1***	2,262	2
Pde2a	***PDE2A***	2,808	2
Ccdc39	***CCDC39***	2,814	3
Tmem67	***TMEM67***	2,988	2
Armc4	***ARMC4***	3,114	1[a]
Adamts6	***ADAMTS6***	3,351	1[b]
Pcsk5	***PCSK5***	5,634	2
Plxnd1	***PLXND1***	5,778	2
Cep290	***CEP290***	7,440	2
Pkd1l1	***PKD1L1***	7,824	2
Megf8	***MEGF8***	8,370	2
Dnah11	***DNAH11***	13,467	8
Dnah5	***DNAH5***	13,866	9

[a] Identical mutation was recovered from two different mutant lines.

[b] Identical mutation was recovered from three different mutant lines, later confirmed to be a spontaneous mutation in the support colony.

Extended Data Table 2
Ciliome Mutations in Laterality and Non-Laterality Lines

Laterality Mutant Lines (30)		Non-Laterality Mutant Lines (31)	
Ciliome Genes*	Non-Ciliome Genes	Ciliome Genes	Non-Ciliome Genes
Anks6	*Aplbl*	*CepllO*	*Acan*

Author Manuscript Author Manuscript Author Manuscript Author Manuscript

Laterality Mutant Lines (30)		Non-Laterality Mutant Lines (31)	
Ciliome Genes*	**Non-Ciliome Genes**	**Ciliome Genes**	**Non-Ciliome Genes**
Armc4 (m)	*Cfcl*	*Dctn5*	*Adamts6*
Bice I	*Cml5*	*Fuz*	*Ap2bl*
Cc2d2a	*Gm572*	*Jbtsll*	*Cxcr4*
Ccdcl51 (m)	*Meg/8*	*Kif7*	*Dnm2*
Cede3 9 (m)	*Mmp21*	*Lrp2*	*Frem2*
Cep290	*Pcsk5*	*Lox*	*Hectdl*
Daw1 (m)	**Total: 7**	*MyhlO*	*Lrpl*
Dnaaf3 (m)		*Pde2a*	*Ltbpl*
Dnah5 (m)		*Pkdl*	*Ndstl*
Dnah11(m)		*Sufu*	*Plxnd1*
Dnail (m)		**Total: 11**	*Prdml*
Drc1 (m)			*Prickle 1*
Dync2hl			*Ptkl*
Dyxlcl (m)			*Robol*
Foxjl (m)			*Smad6*
Iftl40			*Smarca4*
Ift74			*Snx17*
Nek8			*Tabl*
Pkdlll (m)			*Zbtbl4*
Pskhl			**Total: 20**
Tbcld32			
Tmem67			
Total: 23 (12)			

* m: mutation affects motile cilia function

Extended Data Table 3
Mouse CHD genes and associated human diseases

Ciliopathy Related	
Armc4	Primary ciliary dyskinesia, Kartagener Syndrome
Ccdc39	Primary ciliary dyskinesia, Kartagener Syndrome
Dnaaf3	Primary ciliary dyskinesia, Kartagener Syndrome
Dnahl1	Primary ciliary dyskinesia, Kartagener Syndrome
Dnah5	Primary ciliary dyskinesia, Kartagener syndrome
Dnail	Primary ciliary dyskinesia, Kartagener syndrome
Drc1	Primary ciliary dyskinesia, Kartagener syndrome
Dyx1c1	Primary ciliary dyskinesia, Kartagener syndrome
Cc2d2a	Joubert Syndrome; COACH syndrome
Cep290	Joubert Syndrome 5; Senior-loken Syndrome6, Bardet Biedl Syndrome Leber Congenital Amaurosis 10, Meckel Syndrome-4
Jbts17	Joubert Syndrome

Author Manuscript Author Manuscript Author Manuscript Author Manuscript

Ciliopathy Related	
Kif7	Joubert Syndrome, Acrocallosal Syndrome, Hydrolethalus Syndrome
Tmem67	Joubert Syndrome; Nephronophthisis-11, Meckel Syndrome, COACH syndrome, Bardet Biedl Syndrome
Anks6	Polycystic kidney disease; nephronophthisis 16
Bicc1	Polycystic kidney disease; cystic renal dysplasia
Nek8	Polycystic kidney disease; nephronophthisis 9
Pkd1	Polycystic kidney disease
Pkd1l1	Kidney disease, diaphanospondylodysostosis
Dync2h1	Short rib Polydactyly; asphyxiating thoracic dystrophy
Ift140	Mainzer-Saldino Syndrome, short rib thoracic dysplasia
Other Human Diseases	
Ap2b1	Ataxia telangiectasia, cerebellar degeneration
Cfc1	Conotruncal heart defects associated with heterotaxia
Cxcr4	WHIM Syndrome
Dnm2	Charcot-Marie-Tooth Syndrome, Centronuclear myopathy
Frem2	Fraser's Syndrome, Cryptophthalmos syndrome
Lrp1	Alzheimer Disease, Schizophrenia
Lrp2	Donnai-Barrow Syndrome; Facio-oculo-acoustico-renal (FOAR)
Ltbp1	Pseudoexfoliation Syndrome
Megf8	Carpenter's syndrome
Pcsk5	VACTERL/VATER syndrome
Prdm1	Devic disease, B cell lymphoma
Smad6	Aortic valve disease
Smarca4	Rhabdoid tumor predisposition syndrome type 2 (RTPS2), Coffm-Siris syndrome
Snx17	Cerebral cavernous malformation; cavernous malformation
Sufu	Medulloblastoma, basal cell nevus syndrome

Supplementary Material

Refer to Web version on PubMed Central for supplementary material.

Acknowledgments

We thank Ricardo Ramirez for early assistance with the mutagenesis breeding pipeline, Ramiah Subramanian and Deborah Farkas for early assistance with necropsy and pathology examination of mutants, Ashok Srinivasan for early assistance with exome sequencing, Sarosh Fatakia for assistance with sequencing data maintenance, Margaret Wong and Cassandra Krise for assistance with mouse curation. Bruce Beutler for advice on mapping mutation using intercrosses with C57BL/10J strain and whole mouse exome sequencing analysis, Dan Weeks and Ying Shan for assistance in statistical modeling of target gene size estimates, Betsy Goldmuntz for helpful discussions and critical review of the manuscript, New England Research Institutes (NERI) for constructing the CHD Mouse Mutation Database. The project was supported by Award Numbers U01HL098180 (CWL) and U01HL098188 (NERI) from the National Heart, Lung, and Blood Institute, R01MH094564 (MKG) from the National Institute of Mental Health, and HG000330 (JE) from the National Human Genome Research Institute. Funding was also provided by the University of Pittsburgh School of Medicine. The content is solely the responsibility of the authors and does not necessarily represent the official views of the National Heart, Lung, and Blood Institute, the National Human Genome Research Institute or the National Institutes of Health.

Author Manuscript Author Manuscript Author Manuscript Author Manuscript

References

1. Reller MD, Strickland MJ, Riehle-Colarusso T, Mahle WT, Correa A. Prevalence of congenital heart defects in metropolitan Atlanta, 1998-2005. The Journal of pediatrics. 2008; 153:807–813.10.1016/j.jpeds.2008.05.059 [PubMed: 18657826]
2. Hoffman JI. Incidence of congenital heart disease: II. Prenatal incidence. Pediatric cardiology. 1995; 16:155–165. [PubMed: 7567659]
3. Tennstedt C, Chaoui R, Korner H, Dietel M. Spectrum of congenital heart defects and extracardiac malformations associated with chromosomal abnormalities: results of a seven year necropsy study. Heart. 1999; 82:34–39. [PubMed: 10377306]
4. Oyen N, et al. Recurrence of congenital heart defects in families. Circulation. 2009; 120:295–301.10.1161/CIRCULATIONAHA.109.857987 [PubMed: 19597048]
5. Zaidi S, et al. De novo mutations in histone-modifying genes in congenital heart disease. Nature. 2013; 498:220–223.10.1038/nature12141 [PubMed: 23665959]
6. Liu X, et al. Interrogating congenital heart defects with noninvasive fetal echocardiography in a mouse forward genetic screen. Circulation Cardiovascular imaging. 2014; 7:31–42.10.1161/CIRCIMAGING.113.000451 [PubMed: 24319090]
7. Atkinson DE, Drant S. Diagnosis of heterotaxy syndrome by fetal echocardiography. The American journal of cardiology. 1998; 82:1147–1149. A1110. [PubMed: 9817503]
8. Berg C, et al. Prenatal diagnosis of cardiosplenic syndromes: a 10-year experience. Ultrasound in obstetrics & gynecology : the official journal of the International Society of Ultrasound in Obstetrics and Gynecology. 2003; 22:451–459.10.1002/uog.904
9. Taketazu M, Lougheed J, Yoo SJ, Lim JS, Hornberger LK. Spectrum of cardiovascular disease, accuracy of diagnosis, and outcome in fetal heterotaxy syndrome. The American journal of cardiology. 2006; 97:720–724.10.1016/j.amjcard.2005.09.119 [PubMed: 16490445]
10. Tan SY, et al. Heterotaxy and complex structural heart defects in a mutant mouse model of primary ciliary dyskinesia. The Journal of clinical investigation. 2007; 117:3742–3752.10.1172/JCI33284 [PubMed: 18037990]
11. Leigh MW, et al. Clinical and genetic aspects of primary ciliary dyskinesia/Kartagener syndrome. Genetics in medicine : official journal of the American College of Medical Genetics. 2009; 11:473–487.10.1097/GIM.0b013e3181a53562 [PubMed: 19606528]
12. Shiratori H, Hamada H. The left-right axis in the mouse: from origin to morphology. Development. 2006; 133:2095–2104.10.1242/dev.02384 [PubMed: 16672339]
13. Damerla RR, et al. Ion Torrent sequencing for conducting genome-wide scans for mutation mapping analysis. Mammalian genome : official journal of the International Mammalian Genome Society. 2014; 25:120–128.10.1007/s00335-013-9494-7 [PubMed: 24306492]
14. Coghill EL, et al. A gene-driven approach to the identification of ENU mutants in the mouse. Nature genetics. 2002; 30:255–256.10.1038/ng847 [PubMed: 11850622]
15. Bultman S, et al. A Brg1 null mutation in the mouse reveals functional differences among mammalian SWI/SNF complexes. Molecular cell. 2000; 6:1287–1295. [PubMed: 11163203]
16. Kasarskis A, Manova K, Anderson KV. A phenotype-based screen for embryonic lethal mutations in the mouse. Proceedings of the National Academy of Sciences of the United States of America. 1998; 95:7485–7490. [PubMed: 9636176]
17. Chen J, Knowles HJ, Hebert JL, Hackett BP. Mutation of the mouse hepatocyte nuclear factor/forkhead homologue 4 gene results in an absence of cilia and random left-right asymmetry. The Journal of clinical investigation. 1998; 102:1077–1082.10.1172/JCI4786 [PubMed: 9739041]
18. Sung CH, Leroux MR. The roles of evolutionarily conserved functional modules in cilia-related trafficking. Nature cell biology. 2013; 15:1387–1397.10.1038/ncb2888 [PubMed: 24296415]
19. Gray RS, et al. The planar cell polarity effector Fuz is essential for targeted membrane trafficking, ciliogenesis and mouse embryonic development. Nature cell biology. 2009; 11:1225–1232.10.1038/ncb1966 [PubMed: 19767740]
20. Fliegauf M, Benzing T, Omran H. When cilia go bad: cilia defects and ciliopathies. Nature reviews Molecular cell biology. 2007; 8:880–893.10.1038/nrm2278 [PubMed: 17955020]

Author Manuscript Author Manuscript Author Manuscript Author Manuscript

21. Ware SM, Aygun MG, Hildebrandt F. Spectrum of clinical diseases caused by disorders of primary cilia. Proceedings of the American Thoracic Society. 2011; 8:444–450.10.1513/pats.201103-025SD [PubMed: 21926397]

22. Clement CA, et al. TGF-beta signaling is associated with endocytosis at the pocket region of the primary cilium. Cell reports. 2013; 3:1806–1814.10.1016/j.celrep.2013.05.020 [PubMed: 23746451]

23. Sang L, et al. Mapping the NPHP-JBTS-MKS protein network reveals ciliopathy disease genes and pathways. Cell. 2011; 145:513–528.10.1016/j.cell.2011.04.019 [PubMed: 21565611]

24. Stagner EE, Bouvrette DJ, Cheng J, Bryda EC. The polycystic kidney disease-related proteins Bicc1 and SamCystin interact. Biochemical and biophysical research communications. 2009; 383:16–21.10.1016/j.bbrc.2009.03.113 [PubMed: 19324013]

25. Hoff S, et al. ANKS6 is a central component of a nephronophthisis module linking NEK8 to INVS and NPHP3. Nature genetics. 2013; 45:951–956.10.1038/ng.2681 [PubMed: 23793029]

26. Donoso M, et al. Polarized traffic of LRP1 involves AP1B and SNX17 operating on Y-dependent sorting motifs in different pathways. Molecular biology of the cell. 2009; 20:481–497.10.1091/mbc.E08-08-0805 [PubMed: 19005208]

27. Shen Y, et al. Cardiovascular phenotyping of fetal mice by noninvasive high-frequency ultrasound facilitates recovery of ENU-induced mutations causing congenital cardiac and extracardiac defects. Physiological genomics. 2005; 24:23–36.10.1152/physiolgenomics.00129.2005 [PubMed: 16174781]

28. Kim AJ, et al. Microcomputed tomography provides high accuracy congenital heart disease diagnosis in neonatal and fetal mice. Circulation Cardiovascular imaging. 2013; 6:551–559.10.1161/CIRCIMAGING.113.000279 [PubMed: 23759365]

29. Inglis PN, Boroevich KA, Leroux MR. Piecing together a ciliome. Trends in genetics : TIG. 2006; 22:491–500.10.1016/j.tig.2006.07.006 [PubMed: 16860433]

30. Maere S, Heymans K, Kuiper M. BiNGO: a Cytoscape plugin to assess overrepresentation of gene ontology categories in biological networks. Bioinformatics. 2005; 21:3448–3449.10.1093/bioinformatics/bti551 [PubMed: 15972284]

Author Manuscript Author Manuscript Author Manuscript Author Manuscript

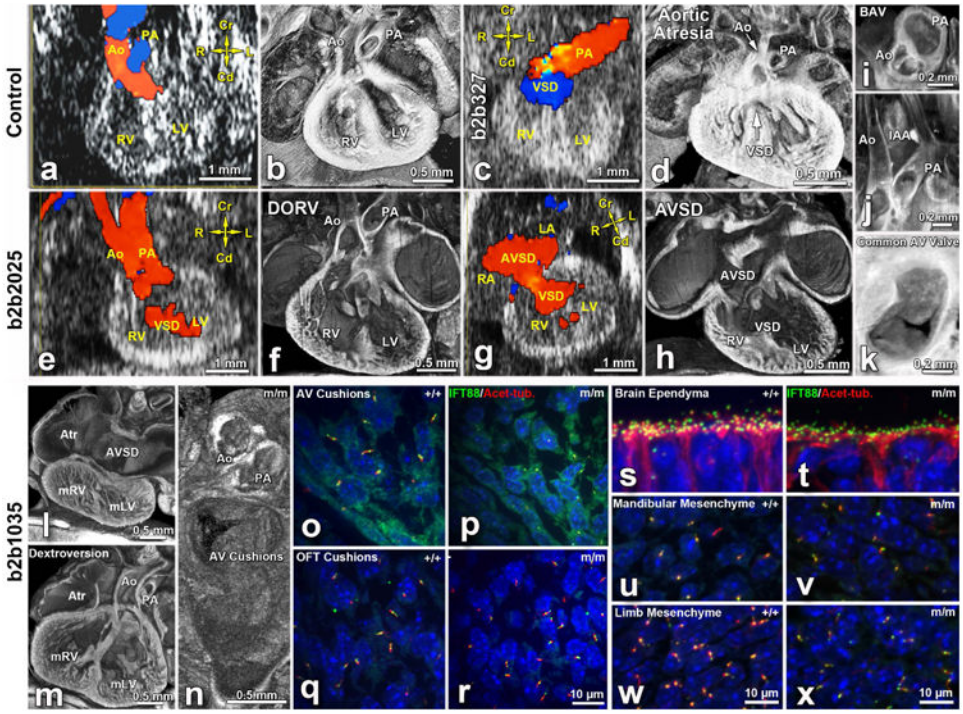

Figure 1. Ultrasound diagnoses of CHD and cilia defects in CHD mutants

Vevo 2100 color flow imaging showed criss-crossing of blood flow indicating normal aorta (Ao) and pulmonary artery (PA) alignment (a, Supplemental Movie S1), confirmed by histopathology (b). E16.5 mutant (line b2b327) exhibited blood flow pattern indicating single great artery (PA) and ventricular septal defect (VSD) (c, Supplemental Movie S2), suggesting aortic atresia with VSD, confirmed by histopathology (d). Color flow imaging of E15.5 mutant (line b2b2025) with heterotaxy (stomach on right; Supplemental Movie S3c) had side-by-side Ao/PA with Ao emerging from right ventricle (RV), indicating DORV/VSD (e,f,Supplemental Movie S3a), and presence of AVSD (g,h,Supplemental Movie S3b,S3c). Histopathology also showed bicuspid aortic valve (BAV,i), interrupted aortic arch (IAA,j), and common AV valve (k). (l-n). *Cc2d2a* mutant exhibits dextrocardia with ventricular inversion (dextroversion) (m), and AVSD (l) with malformed AV cushions (n), but normal outflow cushions. (o-x). Confocal imaging of E12.5 *Cc2d2a* mutant (m/m) vs. wildtype (+/+) embryo sections showed no cilia in AV cushion (o,p), but normal ciliation in outflow cushion (q,r). Fewer and shorter cilia were observed in other mutant embryo tissues (s-x). Red:acetylated tubulin;green:IFT88.

Author Manuscript Author Manuscript Author Manuscript Author Manuscript

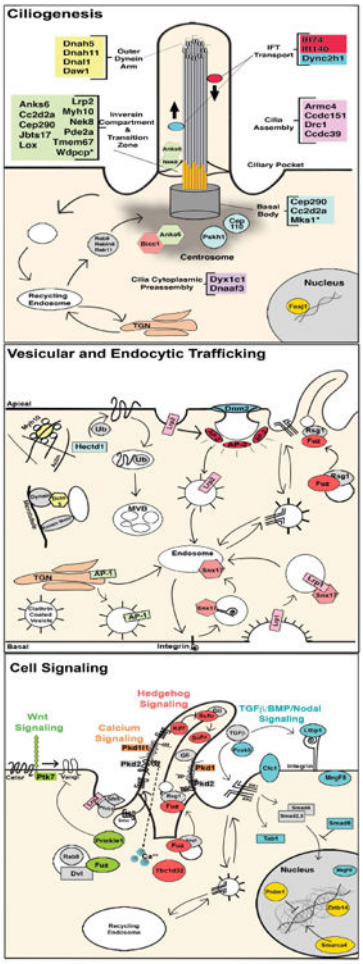

Figure 2. Congenital heart disease genes recovered from mouse mutagenesis screen

Diagrams illustrate biological context of CHD gene function (color-highlighting indicate CHD genes recovered; asterisk denote CHD genes recovered from previous screen[27]). For clarity, ciliome genes (*Dctn5*,*Fuz*) with endocytic function and/or involved in cilia-transduced signaling were not shown in the ciliogenesis panel.

Author Manuscript Author Manuscript Author Manuscript Author Manuscript

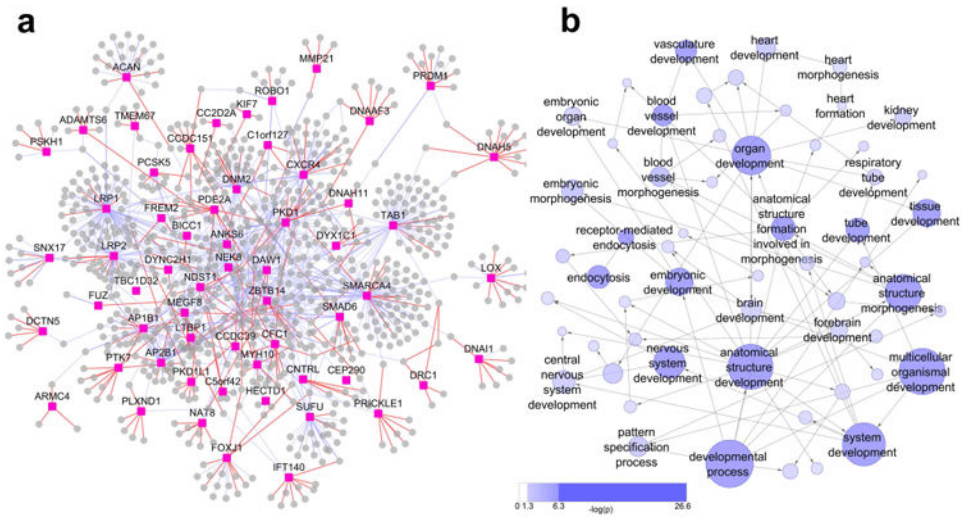

Figure 3. Interactome network of CHD genes with known and predicted interactors

An interactome network was constructed (a) comprising the 61 CHD genes (magenta squares) and their known (blue edges) and predicted (red edges) interactions. The CHD interactome yielded significant enrichment of GO terms related to developmental processes. Circle size proportional to number of genes associated with GO terms.